High power active *X*-band pulse compressor using plasma switches

A. L. Vikharev,[1,2] A. M. Gorbachev,[1,2] O. A. Ivanov,[1,2] V. A. Isaev,[1] S. V. Kuzikov,[1] M. A. Lobaev,[1] J. L. Hirshfield,[2,3] S. H. Gold,[4] and A. K. Kinkead[5]

[1]*Institute of Applied Physics RAS, Nizhny Novgorod, 603600 Russia*
[2]*Omega-P, Inc., New Haven, Connecticut 06510, USA*
[3]*Department of Physics, Yale University, New Haven, Connecticut 06511, USA*
[4]*Plasma Physics Division, U.S. Naval Research Laboratory, Washington D.C. 20375, USA*
[5]*Icarus Research, Bethesda, Maryland 20814, USA*

(Received 13 February 2009; published 30 June 2009)

Results obtained in several experiments on active rf pulse compression at *X* band using a magnicon as the high-power rf source are presented. In these experiments, microwave energy is stored in high-Q TE_{01} and TE_{02} modes of two parallel-fed resonators, and then discharged using switches activated with rapidly fired plasma discharge tubes. Designs and high-power tests of several versions of the compressor are described. In these experiments, coherent pulse superposition was demonstrated at a 5–9 MW level of incident power. The compressed pulses observed had powers of 50–70 MW and durations of 40–70 ns. Peak power gains were measured to be in the range of 7:1–11:1 with efficiency in the range of 50%–63%.

DOI: 10.1103/PhysRevSTAB.12.062003 PACS numbers: 84.40.Az

I. INTRODUCTION

Present interest in microwave pulse compression is motivated primarily by the necessity to obtain high-power, short-duration pulses for rf drive applications in a possible future electron-positron supercollider. Pulse compression can be achieved by either passive or active means, with an expectation for the latter of obtaining higher power gains than with the former without much diminution in efficiency. Until recently, the goal of most studies was passive compression. Passive compressors contain no elements with time-dependent electrodynamic parameters, but do require rapid phase modulation within the incident pulse. Passive compression has been successfully realized in systems of binary pulse compressors (BPCs) [1] and resonance delay lines (SLED-II) [2–4]. In these devices, pulse compression is achieved by rapid reversal of the phase at the klystron that excites a resonator or long delay line. Passive compressors of the SLED-II type generally provide peak power gains in the range of 3–6, with energy efficiency in the range of 50%–70%, while BPCs offer higher efficiency but are generally impractical because of their greater size and cost.

Active compression makes it possible in principle to achieve higher power gains while retaining high efficiency, as compared with passive compression. Active compression is based on the storage of energy in a high-Q microwave resonator and followed by the rapid increase of the coupling between the resonator and the load (Q switching) using the active element, a fast switch. Operation of switches considered for application in the cm-wave band is based on several distinctive approaches, including: (1) changes in the dielectric permittivity (i.e. rf conductivity) of semiconductors, caused by incident pulsed optical radiation [5,6]; (2) generation of pulsed plasma in the switch [7,8]; and (3) injection of a pulsed electron beam [9]. Switching based on changes in magnetic permeability is usually not considered practical, due to the inherent slow switching time of most magnetic circuits. The best experimental results obtained so far have been for *X*-band compressors employing plasma switches, though the parameters achieved are still far from those required for accelerator applications. Power levels are limited principally by the occurrence of multipactor discharges on the surface of dielectrics or semiconductors located within the switch or by electric breakdown at or near the materials used in the switches. Indeed, most switch designs involve the somewhat contradictory requirements that the electric field on the surface of a dielectric element (such as a quartz tube in which a plasma discharge is to be ignited) should be sufficiently low to avoid spontaneous breakdown, but also sufficiently high to guarantee efficient switching when triggered breakdown is initiated.

The resonators used to store microwave energy in the first reported active pulse compressors employed regular rectangular single-mode waveguides. The rf energy was released by means of interference switches, namely, electrically controlled or self-breakdown-driven waveguide H junctions [7,10]. Significant drawbacks of such compressors were the low Q factors of the resonators and the low breakdown thresholds of the switches in the short wavelength range (wavelength $\lambda \leq 3$ cm). Usually, the peak powers achieved in the 3-cm wavelength band did not exceed several megawatts.

Better performance can be expected with compressors that employ oversize electrodynamic structures and distributed switches. To accommodate high rf powers, the energy-storage cavities should have broad cross section, and the electric field at the compressor walls should be

minimized. From this viewpoint, the most attractive choice appears to be a resonator with axial symmetry that operates in low loss TE_{on} modes, whose electric field pattern is a ring structure with zero amplitude at the metallic walls. The main problem that arises when multimode systems are used is the development of a high-efficiency, electrically robust, fast-acting (~ 10 ns) switch to rapidly change the resonator coupling and thus to switch out energy from the storage resonator to the load.

This paper presents results of studying an active two-channel compressor based on oversized cylindrical resonators with novel plasma switches. Designs and high-power tests of two versions of the plasma switch and pulse compressor are described. The compressor utilizes an oversized cylindrical resonator operating in either the TE_{01} or TE_{02} axisymmetric breakdown-proof mode and a reflector containing gas-filled switch tubes that can be externally discharged by application of a high-voltage pulse. Both channels of the two-channel compressor are connected to the rf driver and the load using a 3-dB hybrid coupler. A two-channel arrangement, in contrast to a single channel, allows the isolation of the generator from the power reflected during energy storage without requiring the use of a high power, vacuum compatible circulator, which has not yet been developed, and also results in lower rf electric field in the gas-discharge tube region of the switches.

II. TWO-CHANNEL ACTIVE RF PULSE COMPRESSOR WITH COMBINED INPUT/OUTPUT, OPERATING IN THE TE_{01} MODE

Let us consider briefly the general concept of operation of the two-channel compressor using plasma switches, using as an example an *X*-band (11.43 GHz) compressor with combined microwave input/output element [11,12]. Note that the use of a plasma switch as the energy input/output element makes it possible to change the coupling between the storage resonator and the feed line, and therefore to optimize the efficiency of energy storage in the compressor. A schematic of the two-channel active pulse compressor is shown in Fig. 1. In this design, the microwave power produced by the magnicon generator [item (1) in the figure] is divided equally by means of a 3-dB coupler (3) and is fed into two identical channels in the TE_{10} mode of a rectangular waveguide. Each channel is a single-channel compressor excited in the TE_{01} mode of a circular waveguide. The channel includes a TE_{10} rectangular to TE_{01}° mode converter (6), which is connected via a smooth transition to the storage resonator formed by an electrically controlled reflector (7) and circular-waveguide section (8) with an overcritical narrowing at its end (9). The central part of the cavity for storing microwave energy is a section of an oversized 110-cm-long waveguide 80 mm in diameter, which is equipped with a tapered 40-cm-long transition to a narrower waveguide. The diameter of the latter waveguide is 55 mm, at which the TE_{01}° mode is the only propagating mode of all the axially symmetric modes at 11.43 GHz. Each channel is tuned to the operating frequency by changing the length of the corresponding storage resonator using a special movable taper (12). The loaded Q factor is $Q_L = Q_0 Q_e/(Q_0 + Q_e)$, where Q_0 is the Ohmic Q factor. It is largely determined by the value Q_e of the coupling between the resonators and the waveguide line, and can be controlled by changing the tuning of output reflector (7). The compressor is switched from the energy-storage regime into the energy-release regime by means of electrically controlled plasma switches.

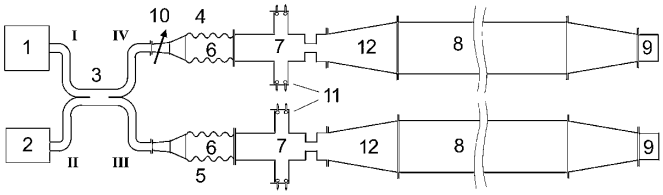

FIG. 1. Schematic diagram of the two-channel active compressor operating in the TE_{01}° mode: (1) driving generator; (2) load; (3) 3-dB hybrid coupler; (4) first channel; (5) second channel; (6) TE_{01}-mode converter; (7) input/output electrically controlled reflector (8) storage cavity; (9) reflector; (10) phase shifter; (11) gas-discharge tubes; (12) movable taper.

The input-output reflector (plasma switch) consists of active and passive sections, as sketched in Fig. 2. The active section is based on stepwise widening of a circular waveguide. The diameter of the wider waveguide is 140 mm; it can excite axially symmetric modes with high-order radial indices. This active section comprises a cylindrical TE_{041} mode resonator containing one or two quartz ring-shaped gas-discharge tubes. The use of two tubes allows one to increase the plasma volume in the resonator and to locate the tubes in an area of weaker microwave field, thereby improving the electric strength of the switch. Each tube is equipped with electrodes to feed in high-voltage pulses and nozzles for gas pumping, which are installed at diametrically opposed positions. The passive portion is a waveguide section with an overcritical narrowing (diaphragm). This passive section makes it possible to reduce the intensity of the rf electric field in the region of the gas-discharge tubes in the active section. By changing the dimensions of the diaphragm in the passive section, one can change the transmission coefficient and thus control the amplitude and duration of the compressed pulse.

The operation of the plasma switch was modeled numerically using the finite-difference time-domain (FDTD) method [13] based on directly solving Maxwell's equations in cylindrical coordinates for the rf electric and magnetic fields E and H. The switch geometry used in the calculations followed the experimental design shown in Fig. 2. The influence of the plasma was taken into account by

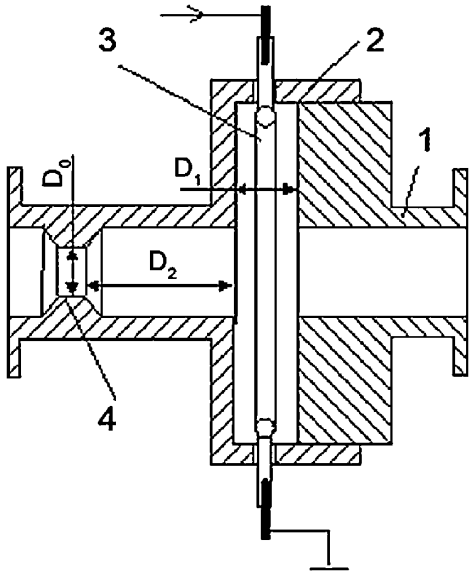

FIG. 2. Plasma switch with active and passive sections, containing one gas-discharge tube: (1) circular waveguide; (2) stepped widening; (3) gas-discharge tube; (4) overcritical narrowing (diaphragm).

introducing conduction currents into the equations, as follows:

$$\nabla \times \vec{E} = -\frac{1}{c} \cdot \frac{d\vec{H}}{dt} \qquad \nabla \times \vec{H} = \frac{\varepsilon}{c} \cdot \frac{d\vec{E}}{dt} + \frac{4\pi}{c}\vec{j}$$
$$\frac{d\vec{j}}{dt} = \frac{e^2}{m} N_e \vec{E} - \nu(N)\vec{j}, \tag{1}$$

where ε is the dielectric permittivity of the quartz tubes, N_e is the electron density, $\vec{j}$ is the current density in the plasma, $\nu(N) = 1.7 \times 10^{-7} N = \text{const}$ is the characteristic rate of electron-molecule collisions with N the density of nitrogen molecules in cm^{-3}, c is the speed of light, and e and m are the charge and mass of the electron, respectively.

In the calculations, we used a standard grid for the FDTD method. The spacing of the grid was chosen in the range from 0.01λ to 0.03λ, where λ is the vacuum wavelength, which ensured the necessary accuracy and high speed of the calculation. When modeling the reflector switching process, we assumed that plasma with some finite electron density was produced instantaneously in the gas-discharge tubes from a gas having a preset density. Gas density and electron density in the quartz tubes were varied in the calculation process. The calculations showed that for efficient switching, the electron density should exceed the critical value $N_e > 10^{12}\ \text{cm}^{-3}$ and that one had to use low gas pressures, $p < 1$ Torr, to reduce the absorption of microwaves in the plasma. In this case, the Ohmic loss in the plasma does not exceed 1%–2%.

The geometrical dimensions of the switch needed to ensure the required switching parameters were determined in the calculation process. The structure of the rf electric field in the switch in the regime of energy storage and energy release from the compressor were obtained by calculations, typical results of which are shown in Fig. 3. It is seen from the figure that the appearance of the plasma in the tubes leads to significantly increased transmission of the TE_{01} wave through the plasma switch.

Calculations showed that the frequency characteristic of the switch has a resonance character and depends significantly on the geometrical dimensions D_0, D_1, and D_2, as identified in Fig. 2. These dimensions were chosen to make overcritical narrowing (4) produce a reflection coefficient in the range $R_d{}^2 = 0.8$–0.9. Combined with the active section, the reflection from the switch amounted to $R^2 \geq 0.99$ in the initial state, and to $R^2 \sim 0.6$–0.7 in the switched state. The calculations showed that, for a microwave power of 400 MW circulating in the resonator, these parameters correspond to a compressed pulse of duration 50–70 ns FWHM and a peak output power of about 100 MW. Note also that the coefficient of microwave reflection from the switch (with a coupling Q-factor Q_e) can be controlled in

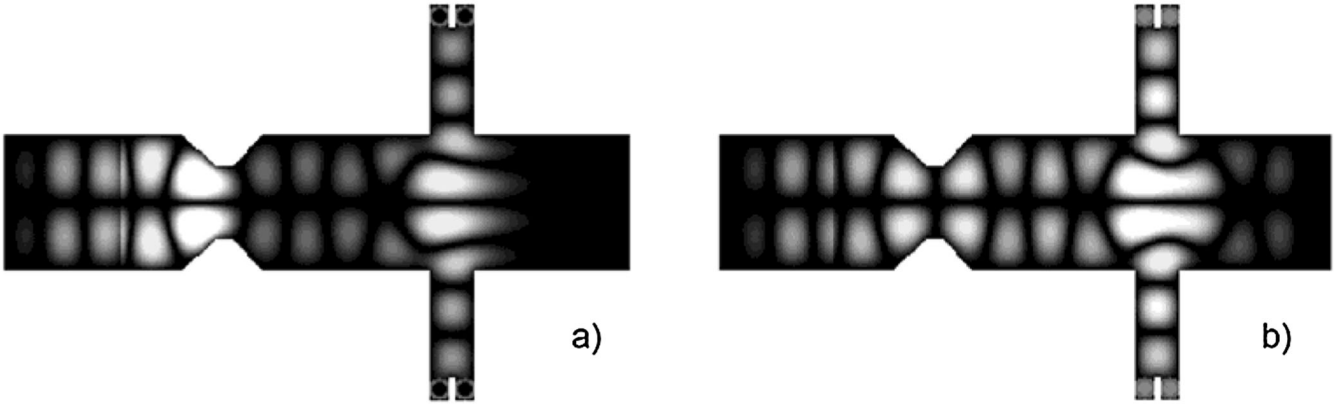

FIG. 3. Instantaneous electric field distributions in plasma switch with two gas-discharge tubes in the (a) energy storage and (b) energy extraction regimes.

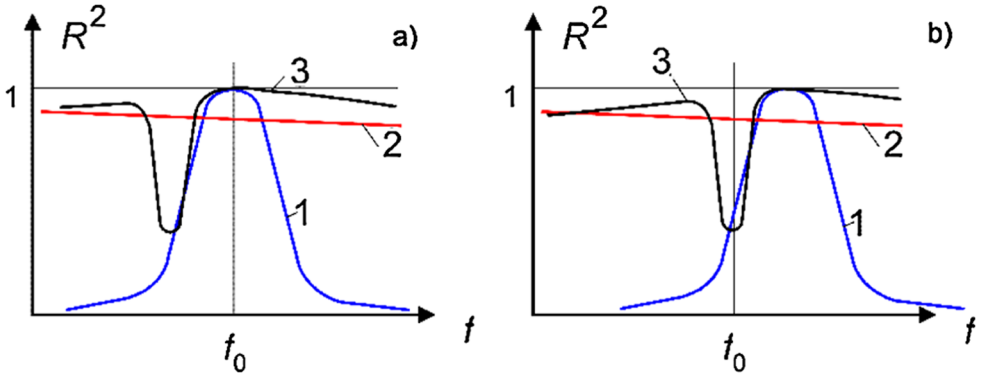

FIG. 4. (Color) Frequency dependence of the reflection coefficient of a plasma switch for (a) the condition of energy storage, and (b) for the condition of energy extraction. Frequency characteristics are shown of (1) the active section, (2) the diaphragm, and (3) total characteristics.

the experiment by changing the length D_1 of the stepwise widening in the active section.

Frequency characteristics of the active section and the diaphragm are shown in Fig. 4, along with the combined characteristic of the plasma switch in the energy-storage regime [Fig. 4(a)] and energy-release regime [Fig. 4(b)]. The principle of operation of the switch is as follows: in the regime of energy storage in the compressor, the resonance frequency of the switch is shifted away from the operating frequency of the compressor (11.43 GHz) and the microwave reflection coefficient from the reflector is close to unity. When high-voltage pulses are applied to the electrodes of the quartz tubes and plasma appears therein, the resonance curve of the switch shifts into the region of the operating frequency of the switch [Fig. 4(b)]. As a result, the microwave transmission coefficient through the switch at a frequency of 11.43 GHz rises to $T^2 \approx 0.3$–0.4, and the energy stored in the compressor goes into the load. Note that the requirement for the electron density at which resonance transmission of the switch is observed is not rigid, since the Q factor of the switch with the plasma is not high, $Q = 150$–200. At the same time, the significant initial detuning of the reflector from the operating frequency of the compressor makes it possible to reduce noticeably the electric fields at the gas-discharge tubes in the regime of energy storage and prevent spontaneous activation of the switch.

Operation of the switch was checked experimentally at low microwave power level in the following way. The switch was tuned to ensure the maximum level of reflected signal observed at the operating frequency $f_0 = 11.43$ GHz and the absence of the signal transmitted through the switch. When a high-voltage pulse was applied to the electrodes and plasma appeared in the gas-discharge tubes, the reflection coefficient decreased and the level of power transmitted through the switch increased. Typical oscillograms of the reflected and transmitted signals, as well as the dependence of the reflection and transmission coefficients on the pressure of nitrogen in the gas-discharge tubes, are shown in Fig. 5.

A 3-dB hybrid coupler is one of the main elements of the two-channel compressor. The coupler makes it possible not only to decouple the generator from the reflected microwave power at the initial stage of energy storage, but also to discharge both channels into one load. The basic idea of the novel quasioptical coupler is to use the effect of image multiplication (Talbot effect) in an oversized rectangular waveguide [14]. This is illustrated in Fig. 6(a). As seen in the figure, a wave beam fed asymmetrically into an oversized rectangular waveguide is split at a certain distance into two beams of equal amplitudes with a phase difference of $\varphi = 90°$. Figure 6(b) shows the frequency characteristics of the developed quasioptical 3-dB hybrid coupler with arm I driven and arm II terminated in a matched load. Curves I and II were obtained with arms III and IV shorted, and show that more than 90% of the reflection from those arms sums into arm II, with only a small reflection back into arm I. Curves III and IV show the balanced splitting of the incident signal at 11.43 GHz into arms III and IV.

High-power tests of the two-channel compressor were carried out at 11.43 GHz using an X-band magnicon [15,16] (with output in the TE_{10}-mode waveguide) with power levels in the range $P_{inc} = 1$–5 MW and pulse duration $\tau = 1$–1.4 μs. A schematic diagram of the experimental setup is shown in Fig. 7. Note that a similar compressor with a combined energy input/output unit, but with a different type of plasma switch, was studied previously [17].

The microwave power fed into port I of the four-port 3-dB hybrid was divided in two and exited through ports III and IV. In the energy-storage regime, the power reflected from the plasma switches into ports III and IV was added in the output port II. In this case, negligible microwave power returned to port I (the electromagnetic waves reflected from each compressor channel were added with opposite phases in this branch). Similar processes took place when

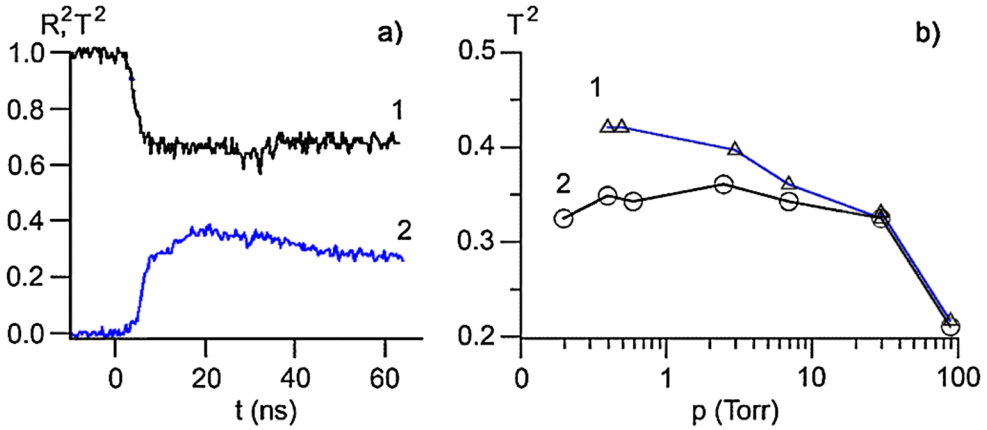

FIG. 5. (Color) (a) Characteristic oscillograms of the reflected and transmitted signals (1 and 2, respectively) for the plasma switch with active and passive sections; (b) dependence of the switch transmission coefficient on the pressure of the gas in the tubes: 1—with one gas-discharge tube, 2—with two gas-discharge tubes.

the compressed pulses were extracted from each of the compressor channels. The phase difference $\Delta\varphi = 0$ required for coherent superposition of the compressed pulses at the inputs of ports III and IV of the 3-dB hybrid coupler was set by using the phase shifter (6) seen in Fig. 7. The output pulse of the compressor went to the matched load (7) through port II. Signals proportional to the power incident on the compressor P_{inc}, the power reflected from the compressor P_{ref} (port I), and the output power P_{com} (port II) were sent into the screen room (10) via directional couplers (8) having coupling coefficients of -55.5 dB using coaxial lines (9). There they were sent to the detectors (12) via the attenuators (11). The signals from the detectors were recorded with a digital oscilloscope. The compressor was pumped down to a pressure of 10^{-6}–10^{-7} Torr by ion pumps (13). The difference between incident and reflected pulses represents the energy stored in the compressor. The share of the energy of the incident microwave pulse that was loaded into the cavities reached 70% in the experiments performed when the compressor tuning was optimum. In this case, the power reflected into the magnicon line did not exceed 1% of the power incident on the compressor.

The compressor was switched from the regime of microwave energy storage into the regime of energy discharge by means of electrically controlled reflectors with two gas-discharge tubes. The pressure of nitrogen in the tubes could be changed externally without disrupting the vacuum in the compressor. The gas discharge was produced simultaneously in the reflectors of both channels by a high-voltage pulse generator (HVPG) (14) that was placed in a shielding box (15) and connected to the compressor via an inductance-free divider limiter (16) that provided a voltage of 60, 80, 90, or 120 kV at the tubes. The trigger pulses (17) went to the modulator of the magnicon (18) and the delay generator (19). From the

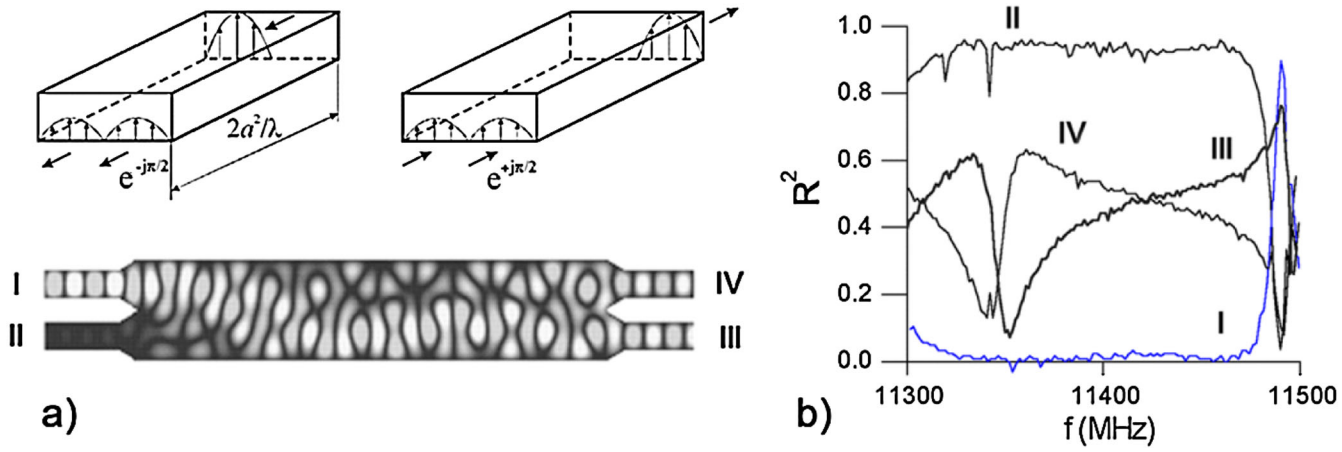

FIG. 6. (Color) Quasioptical 3-dB coupler using the effect of image multiplication: (a) the general concept of operation and instantaneous electric field distribution in the hybrid coupler, with arm I driven and the remaining arms terminated in matched loads; (b) power distribution between arms I to IV in the hybrid coupler (curves I and II are obtained with arms III and IV terminated by reflecting shorts, curves III and IV show the splitting of the incident power from arm I between the two outputs).

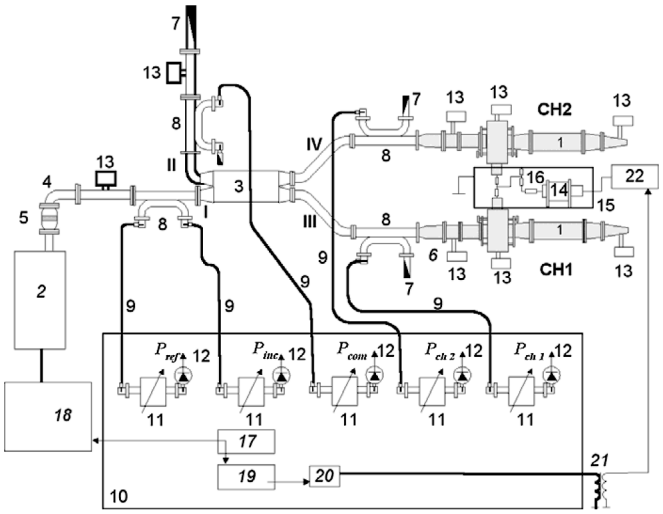

FIG. 7. Schematic diagram of the experimental setup for high-power test of two-channel compressor: (1) single-channel compressor; (2) *X*-band magnicon; (3) quasioptical 3-dB hybrid coupler; (4) waveguide line; (5) output window; (6) phase shifter; (7) matched load; (8) 55.5-dB directional coupler; (9) coaxial cable; (10) screen room; (11) attenuator; (12) detector; (13) ion pump; (14) high-voltage pulse generator; (15) shielding box; (16) divider; (17) trigger generator; (18) modulator; (19) delay generator; (20) trigger amplifier; (21) pulse transformer; (22) high-voltage power supply.

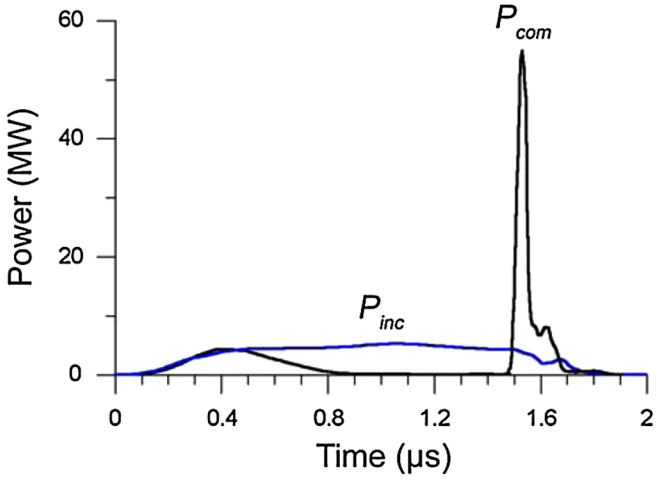

FIG. 8. (Color) Oscilloscope traces of the incident $P_{\rm inc}$ and compressed $P_{\rm com}$ pulses. The gas pressure was 0.4 Torr, the power of the incident pulse 5.1 MW, the peak power of the compressed pulse 53 MW, the pulse duration 43 ns FWHM, and the total compression efficiency 56%.

delay generator, the trigger pulse was sent to the HVPG power supply (22) via the trigger amplifier (20) and a pulse transformer (21). This synchronization scheme made it possible to control the timing of the HVPG pulse with respect to the microwave pulse.

The experiment with coherent composition of the compressed pulses from the two channels into the output port II (Fig. 7) of the compressor was performed via simultaneous gas breakdowns in the tubes of both channels. In the experiment, powers P_1 and P_2 ($P_1 \approx P_2$) of the compressed pulses in each of the channels were measured, as well as the power $P_{\rm com}$ of the total compressed pulse in port II. Experiments showed that simultaneous operation of the switches leads to a sharp increase in the amplitude of the compressed pulse $P_{\rm com} \approx 4P_2$ (gain $= 4$). This is a proof of coherent addition of the compressed pulses from the two channels into the output port II of the quasioptical 3-dB coupler. A typical oscillogram of a compressed pulse obtained when the plasma switch tubes in both channels are fired simultaneously is shown in Fig. 8, along with a trace of the incident pulse. Here the peak power gain is measured to be $>10{:}1$, with the compressed pulse containing 56% of the energy in the incident pulse. The energy in the compressed pulse was calculated by integrating the pulse envelope over the time intervals where the amplitude is greater than 10% of the maximum.

The maximum power of the compressed pulse reached 40–53 MW for pulse durations of 40–60 nsec, depending on the gas pressure in the discharge tubes. In this case, the power gain was in the range 8–11. Total efficiency of the compression in the experiments reached 56%. Good pulse to pulse reproducibility of the shape and amplitude of the compressed microwave pulse was observed. It should also be noted that for the short (~ 1.5 m) storage resonator used in the experiment, the round-trip time along the resonator was equal to $\tau_r \sim 10$ ns, and was comparable with the switching time. Therefore, at the low switch transmission coefficient of $T^2 \sim 0.3$, the energy was extracted from the resonator during the short time interval $t \sim (4\text{–}5)\tau_r$, and the compressed pulse did not have a rectangular shape. Instead, it rose to a maximum in a time determined by the switching time, and then fell off rapidly as the stored energy decayed exponentially. A rectangular output pulse could be obtained by using plasma switches with a higher switch transmission coefficient and a long storage resonator, for instance, with a resonance delay line of the SLED-II type.

III. TWO-CHANNEL PULSE COMPRESSOR USING PLASMA SWITCHES BASED ON MODE CONVERSION, OPERATING IN THE TE_{02} MODE

Another version of an active two-channel pulse compressor in which a plasma switch is employed is based on conversion of the TE_{02}° mode into the TE_{01}° mode. Otherwise, this pulse compressor is similar to the version discussed in Sec. II. In comparison with the first version, this compressor has no input-output reflector, and the plasma switch is placed at the end of the storage resonator. In this case, rf energy is stored in the TE_{02} mode (providing high Q and high breakdown rf electric field) and released in the TE_{01} mode. The operating principle of the switch is based on a sharp increase in the $TE_{02} \rightarrow TE_{01}$ mode con-

version coefficient during plasma generation in a quartz gas-discharge tube built into the switch [18]. The switch possesses resonant properties, which ensures a significant decrease in the electric field strength during energy accumulation in the compressor. The high electric strength of the switch during energy extraction is ensured by placing the discharge tube surface at the node of a standing-wave field formed in the switch. This feature prevents the development of a multipactor discharge on the dielectric surface, which could impose limitations on the switched power.

The design and the principle of operation of one of the two channels of this pulse compressor with the mode conversion switch are shown in Fig. 9. Radiation generated by an rf source in a TE_{10} mode rectangular waveguide is transformed by mode converters (2) and (3) into a TE_{01}° mode and fed to the input of the compressor at a frequency of 11.43 GHz. The compressor consists of coupling device (4) (input and output waveguides, in which the TE_{02} mode is cut off), input horn (5), a 100-cm-long section of cylindrical waveguide (6) with a diameter of 8 cm, and plasma switch (10–15). The input horn, cylindrical waveguide, and plasma switch form a storage cavity for the TE_{02} mode.

The cylindrical waveguide includes a section of variable length, which can be changed using a special mechanical drive in order to tune the cavity to a desired working frequency. In the regime of energy storage, a small fraction ($\sim$ 2%–3%) of the TE_{01} mode supplied from the rf source via the input waveguide is converted with the aid of the plasma switch into the TE_{02} mode. This mode is completely reflected from input horn (5) owing to the supercritical taper down to waveguide (4). As a result, the microwave energy is stored in the cavity in the TE_{02} mode. A compressed pulse generated during plasma switch operation is extracted to load (9) via circulator (1) and detected using directional coupler (7) and detector (8). The plasma switch comprises cone taper (10) connected via round waveguide section (11) with a diameter of 3.8 cm to

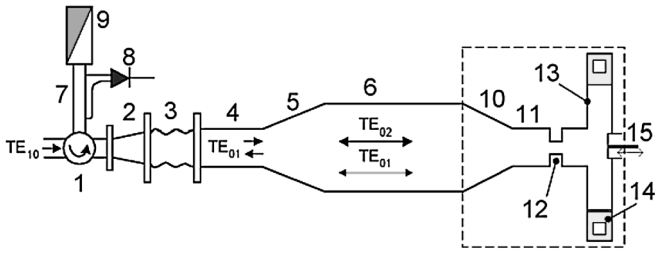

FIG. 9. Schematic diagram of a microwave compressor with plasma switch based on conversion of the TE_{02} mode into the TE_{01} mode: (1) circulator; (2) TE_{10} rectangular to TE_{01}° mode converter; (3) $TE_{11}^{\circ} \rightarrow TE_{01}^{\circ}$ mode converter; (4) input and output waveguides; (5) input horn; (6) cylindrical waveguide cavity; (7) directional coupler; (8) detector; (9) matched load; (10) cone taper; (11) round waveguide section; (12) diaphragm; (13) stepwise widening of circular waveguide; (14) ring-shaped quartz gas-discharge tube; (15) adjusting piston.

diaphragm (12) and stepwise widening of circular waveguide (13), which accommodates a ring-shaped quartz gas-discharge tube (14) of special design with metal electrodes. The discharge tube with a rectangular cross section is milled into a quartz disk, which ensured the fabrication of this part with high precision and uniformity. The reflector volume can be adjusted with the aid of a movable short circuit (15).

The principle of operation of the plasma switch is based on mode conversion (Fig. 10). In the energy-storage regime [Fig. 10(a)], the energy is stored in the TE_{02} mode, which is reflected from the switch with almost no scattering into the TE_{01} mode. The latter is achieved by mutual compensation of two radiation flows. One is formed upon reflection from the cone taper (10) and the other, from diaphragm (12) (Fig. 9). Indeed, reflecting from the cone taper, the TE_{02} mode partly converts into the TE_{01} mode that propagates toward the input horn, while the other part propagates toward the diaphragm. The conversion coefficient is determined by the cone taper parameters. For a given diaphragm, the length of waveguide (11) is adjusted so that TE_{01} waves reflected from the diaphragm and cone taper would add at the compressor output with opposite phases. As a result, the total coefficient of TE_{02}-wave conversion into the TE_{01} wave in the switch amounts to 2%–3%. This coupling coefficient is optimum for energy storage in the cavity when it is excited with 1–2 μs long microwave pulses.

The stepwise widening of the waveguide with a ring-shaped quartz gas-discharge tube and a diaphragm forms a low-Q cavity. The plasma switch operation was simulated using the FDTD method. The dimensions of the stepwise widening of the quartz tube and the diaphragm are selected so that the working frequency at the stage of energy storage would be out of resonance with the switch. When high-voltage pulses are applied to the electrodes, plasma is generated in the quartz tube and the resonance frequency of the switch cavity changes. The frequency shift depends on the electron density in the plasma and the position of the adjusting short. These parameters are selected so that the generation of plasma brings the switch into resonance with the working frequency of the compressor. In resonance, the phase of the TE_{01} wave reflected from the diaphragm changes by 180°, and this wave adds in phase to the wave reflected from the cone taper. As a result, the coefficient of conversion from the TE_{02} mode to the TE_{01} mode increases to 25%–30%, and the microwave energy stored in the cavity in the TE_{02} mode is emitted through the input-output horn in the TE_{01} mode [Fig. 10(b)]. The characteristic switching time is determined by the loaded-Q value of the stepwise widening and amounts to 10–15 ns. It should be noted that the electric field strength in the stepwise widening of the circular waveguide substantially increases when it is shifted into resonance. For this reason, the gas-discharge tube dimensions were calculated to ensure that

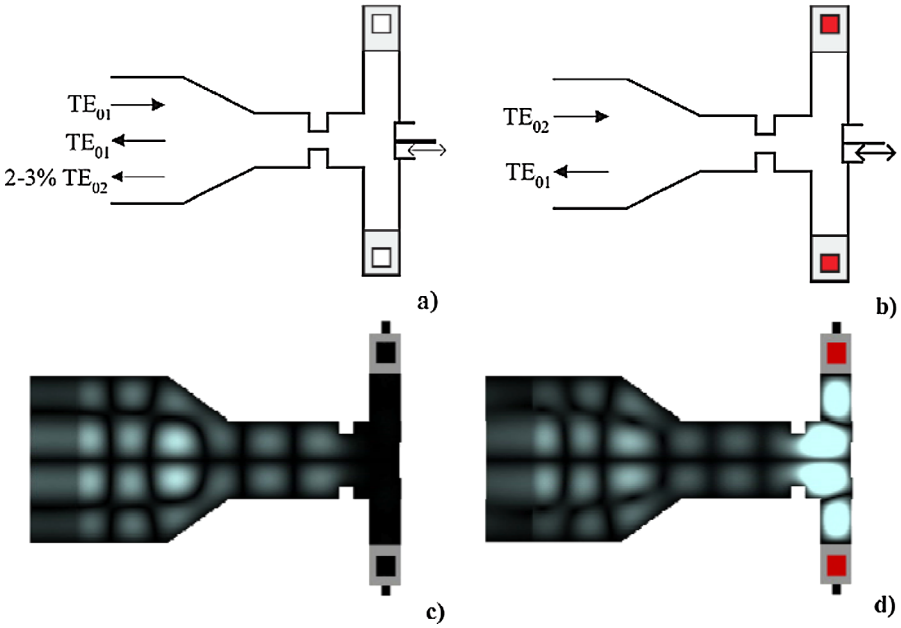

FIG. 10. (Color) Schematic diagrams [(a) and (b)] and instantaneous electric field distribution [(c) and (d)] in the plasma switch based on $TE_{02} \rightarrow TE_{01}$ mode conversion, illustrating switch operation in the (a) and (c) energy storage and (b) and (d) microwave pulse extraction regimes.

its inner surface would occur at the node of the standing-wave field of the mode excited in the switch. Figure 10 shows the typical instantaneous distribution of the mean-square electric field in the switch in the regimes of energy storage and energy extraction from the compressor. As can be seen from Fig. 10(c), the microwave power in the energy accumulation stage is almost completely reflected from the diaphragm. In the regime of microwave pulse extraction, the appearance of plasma in the discharge tube causes the cavity formed by the waveguide section with stepwise widening to tune to the incident wave frequency. As a result, the field amplitude in this cavity sharply increases, but the quartz tube surface still falls at the node of the electric field [Fig. 10(d)].

The intensity of the electric field in the switch during energy storage and the magnitude of electron density at which efficient switching is observed are strongly dependent on the position of adjustment piston (15). The dependence of the mode conversion ratio on the electron density in the gas-discharge tubes is shown in Fig. 11 for different values of the piston position. It is seen that, for each position of the adjustment piston, there is some optimal electron density, at which the switching coefficient reaches the maximum value. The optimal value of the electron density decreases as the piston moves towards the stepwise widening (13). Existence of an optimal electron density is connected with the fact that detuning of the resonance frequency of the adjustment piston decreases with respect to the magnicon frequency when the piston moves inside the switch resonator. When this detuning is small, a lower electron density is required to tune the switch resonator into resonance. When the electron density is excessive, the resonance frequency of the switch changes too strongly and starts to exceed the operating frequency of the compressor significantly. As a result, the switch, as in the case of plasma absence, stays out of resonance and the coefficient of the $TE_{02} \rightarrow TE_{01}$ mode conversion remains comparatively low. Thus, one can achieve the optimal

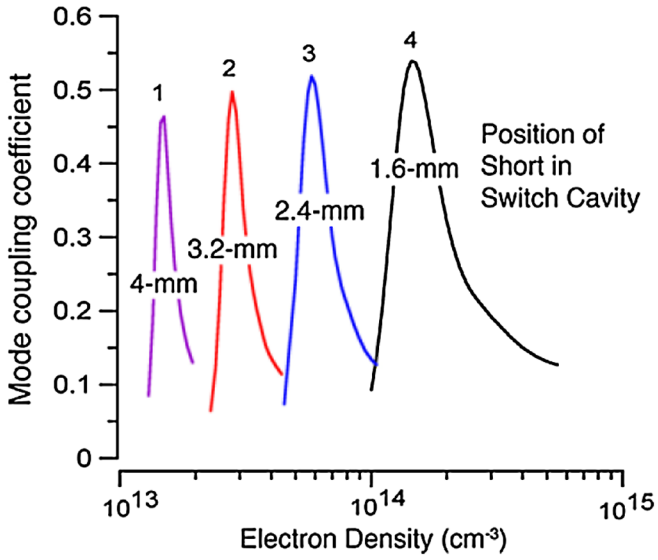

FIG. 11. (Color) Dependence of the coefficient of the TE_{02} to TE_{01} mode conversion on electron density at different position of adjusting short. Curve numbers mark different positions of the adjusting piston in the switch (switch settings).

switching ratio for a given electron density by changing the position of the piston.

The results of calculations showed that, for a circulating power of 400 MW in the resonator, the mean-square electric field strength at the discharge tube surface does not exceed 6.5 kV/cm in the regime of energy accumulation and 35 kV/cm in the regime of microwave pulse extraction. Such electric fields are below the level corresponding to surface discharge thresholds. This makes it possible to reach a peak output power in excess of 100 MW in the compressed pulse.

A schematic diagram and the experimental setup for high-power tests are shown in Fig. 12. The two-channel pulse compressor was excited by a magnicon at a power level of 8–9.4 MW. Higher levels of microwave power in comparison with the experiment described in Sec. II were reached by summing power of two magnicon outputs with a combiner (4) based on a single-mode 3-dB coupler.

Each of the compressor channels was a single-channel compressor (1) with the mode converting plasma switch described above. The storage resonators were formed by a tapered transition (horn) from a diameter of 55 to 80 mm, a cylindrical waveguide 110 cm long and 80 mm in diameter, and the plasma switch. The cylindrical waveguide included a section whose length could be adjusted mechanically. The horn was below cutoff for the TE_{02} mode and propagating for the TE_{01} mode. The energy was fed into the storage resonator via the horn. The energy was fed out via the horn after excitation of the plasma switch. The measured loaded Q factor of each of the channels was $Q_{L1} \approx Q_{L2} \approx 2.3 \times 10^4$. The two compressor channels were connected to the combiner (4) via the single-mode 3-dB hybrid coupler (6). The combiner was connected to the magnicon (3) through windows (5) that separated the vacuums of the magnicon and the compressor. Microwave power fed into port I was divided in two into ports III and IV. In the energy-storage regime, the power reflected from the resonators into ports III and IV was added in the output port II. In this case, no microwave power entered port I (the electromagnetic waves reflected from each compressor channel were added with opposite phases in this branch). The phase difference $\Delta\varphi = 0$ required for division of the input power of the magnicon in two between ports III and IV of the single-mode 3-dB hybrid coupler was set by using the phase shifter (7).

Directional couplers (− 55.5 dB) were installed in each channel of the compressor. They allowed fine-tuning of the channels to the resonance frequency and detection of compressed pulses in each of the channels separately. To eliminate spurious reflections, matched loads were built into port II (8). The signals proportional to the power incident on the compressor P_{inc} and the power reflected from the compressor P_{mag} and P_{com} (ports I and II) were sent into the screen room via directional couplers (9) with coupling coefficients of −55.5 dB and coaxial lines. A similar method was used to register signals P_1 and P_2 at the output of each of the compressor channels. The signals from the detectors were recorded with a digital oscilloscope. The duration of the compressed pulse was determined by the conversion coefficient from the TE_{02} mode to the TE_{01} mode.

A. Untriggered switching regime

Initially, operation of each of the compressor channels was studied separately at high power. Each channel was separately tuned to the magnicon frequency by changing the cavity length using movable tapers (12). The tuning was adjusted to maximize the power loaded into the resonator when the difference of the incident and output power ($P_{inc} - P_{com}$) was maximum. The share of the power of the incident microwave pulse that was loaded into the cavities reached 70%–75% in the experiments performed, when the compressor tuning was optimum.

Experiments showed that the plasma switch could be tuned so that no self-breakdown of the gas in the gas-discharge tubes would occur, and no multipactor discharge would occur on the tube surfaces, for a maximum power from the magnicon of $P \sim 10$ MW. Changing the pressure of nitrogen in the quartz tubes and the position of the

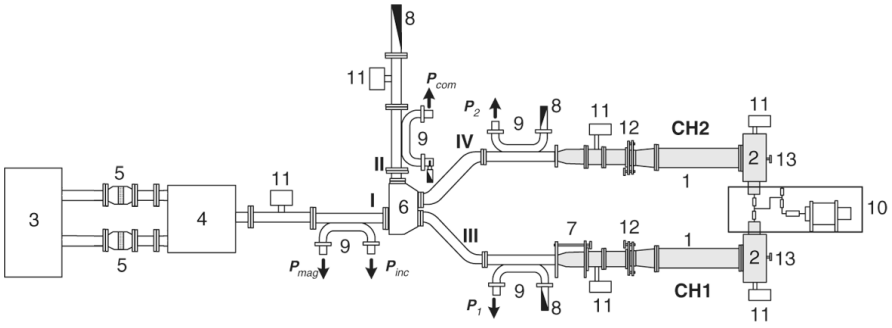

FIG. 12. Schematic diagram of the experimental setup for tests of a two-channel microwave compressor: (1) single-channel of the compressor; (2) plasma switch, based on mode conversion; (3) magnicon; (4) combiner; (5) output window; (6) single-mode 3-dB hybrid coupler; (7) phase shifter; (8) matched load; (9) 55.5-dB directional coupler; (10) high-voltage pulse generator; (11) ion pump; (12) movable taper; (13) adjusting piston.

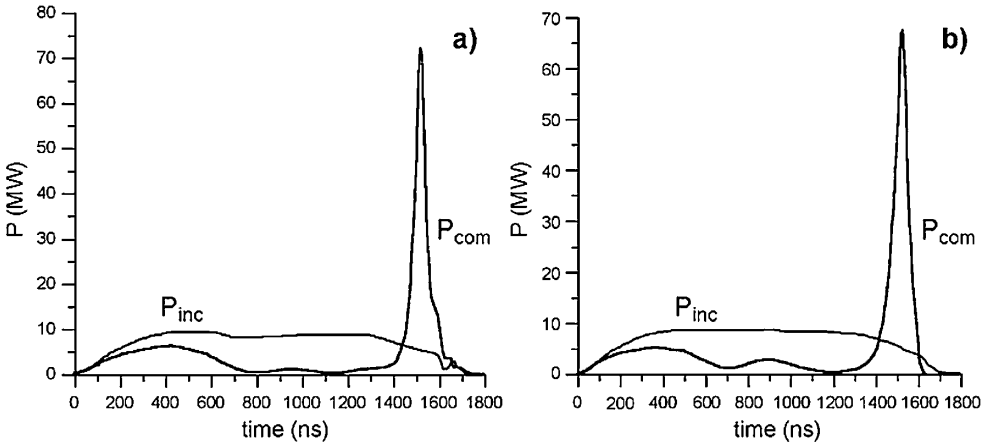

FIG. 13. Sample oscilloscope traces of the incident and compressed pulse for the two-channel compressor with the switch based on mode conversion. The gas pressure in the tubes was 0.04 Torr. (a) Power of the compressed pulse −71 MW, pulse duration −49 ns, peak power gain −8.4:1, power of the incident pulse −8.5 MW; compression efficiency −48%. (b) Power of the compressed pulse −68 MW, pulse duration −69 ns, peak power gain −8:1, power of the incident pulse −8.5 MW; compression efficiency −61%.

adjusting piston of each plasma switch allowed conditions where self-breakdown of the gas occurred at the end of the magnicon pulse simultaneously in the two channels. In this experiment, the pressure in the gas-discharge tubes was varied in the range $p = (2–5) \times 10^{-2}$ Torr. The incident power was 8.5–9 MW, and adjustment of the plasma switch was done such that self-breakdown of the gas in the tubes took place at the end of incident pulse. In this case, pulses compressed in each channel were superimposed with high phase stability in the output of the 3-dB hybrid coupler. Typical oscillograms of compressed pulses obtained when the plasma switch tubes in both channels fired simultaneously are shown in Fig. 13.

The compressed pulses obtained in this untriggered switching regime had peak powers of 65–71 MW at an incident power P_{inc} of 8–9 MW and durations of 45–70 ns. In this case, the maximum power gain measured was 8.7. The total efficiency of the compression in the experiments was ∼55%–63%.

B. Triggered switching regime

Experiments with coherent superposition of the compressed pulses from both channels were also carried out with simultaneous gas breakdowns in the switch tubes triggered by the high-voltage pulse generator, which ionizes gas inside the switch tubes, thus creating an initial electron density that tunes the switch towards resonance. It was found that the electron density $N_e = (1–2) \times 10^{12}$ cm^{-3}, produced at pressures $p = (2–5) \times 10^{-2}$ Torr, was insufficient to switch the compressor when it was tuned to the breakdown-proof regime (position of adjusting short corresponds to curve 3 in Fig. 11). When the switch was tuned to the density produced by the HVPG (position of adjusting short corresponds to a peak to the left of that of curve 1 in Fig. 11), it resulted in shorter lengths of the compressed pulse and incomplete output of the energy from the cavity. Indeed, at the moment of switching, the electric field in the switch increases, and the electron density starts to significantly exceed the density produced by the HVPG. In this case, the shift of the switch resonance frequency starts to exceed the value required for switching. As a result, the electron density passes back out of the switching regime up to $\sim 10^{13}$–10^{14} cm^{-3}, producing transient switching and a short compressed pulse. The compressed pulses obtained in this regime had a power of 25 MW, output pulse length of 30–35 ns, and efficiency about 45% [see Fig. 14(a)].

Therefore, effective switching required keeping the electron density N_e near resonance during the output pulse. There are only two experimental adjustments available for the switching: the gas fill pressure and the adjustable short at the end of the switch. The resonant N_e depends on the initial tuning of the cavity using the adjustable short. The gas fill affects self-breakdown, the initial electron density produced by the HVPG, and the electron density produced by rf fields as the switch tunes into resonance. When the pressure in the tubes increases up to $p = 0.2–0.5$ Torr, the increasing rf fields during switching do not change the electron density produced by the HVPG ($N_e \sim 10^{13}$ cm^{-3}) significantly, so that the switch remains in resonance. In this case, one can achieve stable triggered switching. However, in the experiments, the tuning of the switch under these pressures and electron densities (switch setting corresponding to curve 1 in Fig. 11) led to an increase in rf field at the stage of energy storage, and self-breakdown limited incident power to a few megawatts. The compressed pulses obtained in this regime where not shortened, since the cavity remained in resonance during the switching process, and had a power of ∼8.5 MW,

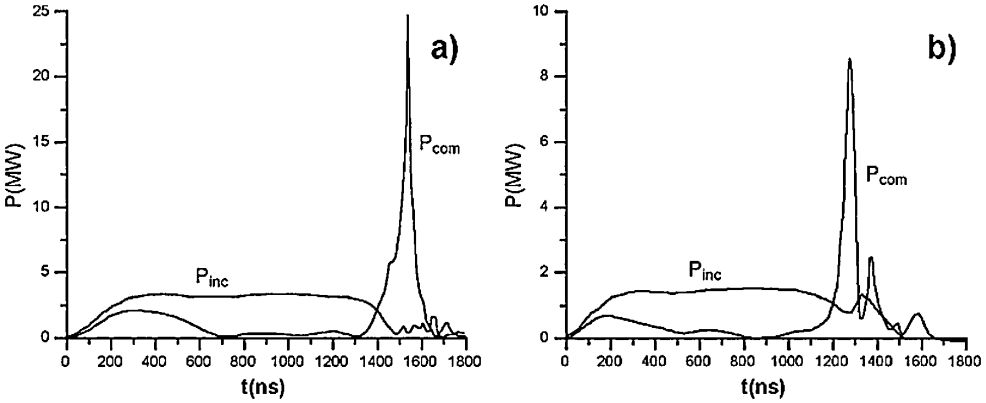

FIG. 14. Oscilloscope traces of the incident and compressed pulse for triggered operation of the two-channel compressor with the switch based on mode conversion. (a) Switch setting corresponding to a peak to the left of curve 1 in Fig. 11, pressure ~0.02–0.05 Torr. (b) Switch setting corresponding to curve 1 in Fig. 11, pressure ~0.2–0.5 Torr.

output pulse length of 53 ns, and efficiency of ~64% [see Fig. 14(b)].

Thus, the experiments performed showed that the switch based on mode conversion allows one to achieve high powers in the compressed pulse, but requires high levels of the electron density to switch it. Therefore, to ensure efficient triggered switching, it will be necessary to modify the cavity of the switch. There are two possible solutions. The first would involve redesigning the switch cavities to reduce the rf electric field at the quartz switch tubes. This approach appears to be feasible, and would permit triggered operation at the 100 MW power level. The second solution would require a major change in the switch design. It would require changing the switching mode to detune the switch cavity out of resonance, rather than tuning it into resonance. The advantage of this second approach is that, unlike the first approach, it does not require producing a certain electron density to cause switching and then maintaining it in a limited range even as the rf electric field in the switch increases substantially during the switching process. Instead, the switch would be closed with the switching cavity in resonance, and switching would only require that the trigger generate sufficient electron density to switch it out of resonance. However, with this approach, a plasma switch tube is not practical, since strong rf electric fields would exist in the switch before the trigger pulse was applied. In this case, an alternative switching mechanism would be to send an electron beam through the switch cavity to tune it out of resonance and accomplish the switching; such an approach is under study.

IV. CONCLUSIONS

This paper reports the results of experiments on two different versions of a two-channel active microwave pulse compressor using plasma switch tubes. One of these stores energy in the TE_{01} mode in a long cylindrical cavity and uses this mode for switching, while the second stores energy in the TE_{02} mode, and uses mode conversion into the TE_{01} mode for switching. Both of these experiments operated in a reflection configuration, in which a 3-dB hybrid coupler is used to separate the input drive pulse from the compressed output pulse. These experiments have demonstrated the coherent addition of the output pulses from the two compressor channels using the hybrid coupler at up to 10 MW of incident power, resulting in compressed pulses with powers of 50–70 MW and durations of 40–70 ns. These pulses were obtained at power gains of 7.4:1 to 11:1 and total energy efficiencies of 55%–63%. While many technical issues remain, these experiments have demonstrated that active pulse compressors using plasma switches are a promising candidate for the high-power pulse compressors that may be needed for future linear colliders operating in the *X* band. Such switches could also be employed in active versions of the SLAC SLED-II pulse compressor [19].

ACKNOWLEDGMENTS

This work was supported by the U.S. Department of Energy, Office of High Energy Physics, and the U.S. Office of Naval Research.

[1] Z. Farkas, IEEE Trans. Microwave Theory Tech. **MTT-34**, 1036 (1986).

[2] P. B. Wilson, Z. D. Farkas, and R. D. Ruth, in *Proceedings of the 1990 Linear Accelerator Conference*, edited by S. Schriber (Los Alamos National Laboratory, Los Alamos, NM, 1991), pp. 204–206; also, SLAC-PUB-5330, 1990 (unpublished).

[3] S. G. Tantawi and C. D. Nantista, in *High Energy Density and High Power RF*, edited by S. H. Gold and G. S. Nusinovich, AIP Conference Proceedings 691 (AIP, Melville, New York, 2003), p. 172.

[4] S. G. Tantawi, C. D. Nantista, V. A. Dolgashev, C. Pearson, J. Nelson, K. Jobe, J. Chan, K. Fant, J. Frisch, and D. Atkinson, Phys. Rev. ST Accel. Beams **8**, 042002 (2005).

[5] S. G. Tantawi, R. D. Ruth, A. E. Vlieks, and M. Zolotorev, IEEE Trans. Microwave Theory Tech. **45**, 1486 (1997).
[6] F. Tamura and S. G. Tantawi, Phys. Rev. ST Accel. Beams **5**, 062001 (2002).
[7] R. A. Alvarez, D. P. Byrne, and R. M. Johnson, Rev. Sci. Instrum. **57**, 2475 (1986).
[8] A. L. Vikharev, O. A. Ivanov, A. M. Gorbachev, V. A. Isaev, S. V. Kuzikov, S. H. Gold, and A. K. Kinkead, in High Energy Density and High Power RF (Ref. [3]), p. 197.
[9] D. L. Birx and D. J. Scalapino, J. Appl. Phys. **51**, 3629 (1980).
[10] A. N. Didenko and Yu. G. Yushkov, *High-Power Microwave Nanosecond Pulses* (Energoatomizdat, Moscow, 1984), in Russian.
[11] A. L. Vikharev, A. M. Gorbachev, O. A. Ivanov, V. A. Isaev, V. A. Koldanov, S. V. Kuzikov, A. G. Litvak, M. I. Petelin, J. L. Hirshfield, and O. A. Nezhevenko, in *Advanced Accelerator Concepts*, AIP Conference Proceedings 569 (AIP, Melville, New York, 2001), p. 741.
[12] A. L. Vikharev, A. M. Gorbachev, O. A. Ivanov, V. A. Isaev, S. V. Kuzikov, J. L. Hirshfield, O. A. Nezhevenko, S. H. Gold, and A. K. Kinkead, Radiophys. Quantum Electron. **46**, 802 (2003).
[13] A. Taflove, *Advances in Computational Electrodynamics. The Finite-Difference Time-Domain Method* (Artech, London, 1998), p. 724.
[14] G. G. Denisov and S. V. Kuzikov, in *Strong Microwaves in Plasmas, Proceedings of the International Workshop*, edited by A. G. Litvak (IAP, Nizhny Novgorod, Russia, 2000), p. 618.
[15] S. H. Gold, O. A. Nezhevenko, V. P. Yakovlev, A. K. Kinkead, A. W. Fliflet, E. V. Kozyrev, R. True, R. J. Jansen, and J. L. Hirshfield, in *High Energy Density Microwaves*, edited by R. M. Phillips, AIP Conference Proceedings 474 (AIP, New York, 1999), p. 179.
[16] O. A. Nezhevenko, V. P. Yakovlev, J. L. Hirshfield, E. V. Kozyrev, S. H. Gold, A. W. Fliflet, A. K. Kinkead, R. B. True, and R. J. Hansen, in *Proceedings of the 1999 Particle Accelerator Conference*, edited by A. Luccio and W. MacKay (IEEE, Piscataway, New Jersey, 2000), Vol. 2, p. 1049.
[17] A. L. Vikharev, A. M. Gorbachev, O. A. Ivanov, V. A. Isaev, V. A. Koldanov, S. V. Kuzikov, J. L. Hirshfield, and S. H. Gold, Radiophys. Quantum Electron. **51**, 597 (2008).
[18] A. L. Vikharev, A. M. Gorbachev, O. A. Ivanov, V. A. Isaev, S. V. Kuzikov, and M. A. Lobaev, Tech. Phys. Lett. **33**, 785 (2007).
[19] A. L. Vikharev, O. A. Ivanov, A. M. Gorbachev, V. A. Isaev, S. V. Kuzikov, V. A. Koldanov, M. A. Lobaev, S. H. Gold, A. K. Kinkead, O. A. Nezhevenko, J. L. Hirshfield, S. Tantawi, and C. Nantista, in *High Energy Density Microwaves*, edited by D. K. Abe and G. S. Nusinovich, AIP Conference Proceedings 807 (AIP, Melville, New York, 2006), p. 463.